ＲＣポリフェーズ・フィルタの解析

- 高次フィルタ伝達関数、ナイキスト線図の導出、寄生容量の影響の解析-

◯山口　宣[†]　小林　春夫[†]　康　剣[†]　仁木　義規[†]　北原　崇[†]

† 群馬大学工学部電気電子工学科　〒 376-8515 群馬県桐生市天神町 1-5-1
E-mail: †k_haruo@el.gunma-u.ac.jp

あらまし　携帯電話等の無線送受信機のアナログフロントエンド部で、直交信号 (I, Q 信号) 発生、イメージ除去のため用いられる RC ポリフェーズ・フィルタの設計論の確立のための解析を行なった。具体的には、１次、２次、３次、４次のフィルタの伝達関数を求め、ナイキスト線図からそれらの特徴を示した。また、寄生容量・負荷容量の伝達関数への影響を示した。

キーワード　ポリフェーズ・フィルタ、イメージ信号除去、RF 回路、無線送受信器、複素信号

Analysis of RC Polyphase Filters

- High-Order Filter Transfer Functions, Nyquist Charts, and Parasitic Capacitance Effects -

◯Nobu YAMAGUCHI[†], Haruo KOBAYASHI[†], Jian KANG[†], Yoshiki NIKI[†], and Takashi KITAHARA[†]

† Dept. of Electronic Engineering, Gunma University　1-5-1 Tenjin-cho, Kiryu 376-8515 Japan
E-mail: †k_haruo@el.gunma-u.ac.jp

Abstract　This paper derives explicit transfer functions for first-, second-, third- and fourth-order RC polyphase filters; these are important components used for image rejection and in quadrature signal generation circuits in the analog front- ends of wireless transceivers. We use Nyquist charts to characterize them, and also discuss the effects of parasitic node capacitances.

Key words　Polyphase Filter, Image Rejection, RF Circuit, Wireless Transceiver, Complex Signal

1. Introduction

RC polyphase filters [1] are important components in analog front-end of wireless transceivers; their roles are described in [2], [3], and their use for In-Phase and Quadrature (I and Q) signal generation and for image rejection is described in [4]〜[8]. Up to now their design has been based on simulation, in most cases [6]. However, in our previous papers [2], [3], we derived explicit transfer functions for first-, second-, and third-order RC polyphase filters, and Fukura et.al. have also derived them [9]. In this paper we analyze their characteristics in more detail; we derive the transfer function of a fourth-order filter, clarify the characteristics of first-, second- and third- order filter with their Nyquist charts, and also study the effects of parasitic capacitances and loading capacitances. In a companion paper [10], we also discuss input impedance, output termination, component mismatch effects and a flat-gain design algorithm for RC polyphase filters.

In this paper, we use the following notation:

$$\omega_k := 1/(R_k C_k), \quad \omega_{ij} := 1/(R_i C_j) \quad (k, i, j = 1, 2, 3, 4).$$

2. Transfer Function

Let us consider the RC polyphase filters in Figs.1, 2, 3 and define the following:

$$I_{in}(t) := I_{in+}(t) - I_{in-}(t), \quad I_{out}(t) := I_{out+}(t) - I_{out-}(t),$$
$$Q_{in}(t) := Q_{in+}(t) - Q_{in-}(t), \quad Q_{out}(t) := Q_{out+}(t) - Q_{out-}(t).$$

Also define complex signals $V_{in}(t)$ and $V_{out}(t)$ as follows [11]:

$$V_{in}(t) := I_{in}(t) + jQ_{in}(t), \quad V_{out}(t) := I_{out}(t) + jQ_{out}(t).$$

Letting $V_{in}(j\omega)$, $V_{out}(j\omega)$, $I_{out}(j\omega)$, $Q_{out}(j\omega)$, $I_{in}(j\omega)$ and

$Q_{in}(j\omega)$ be the Fourier transform of $V_{in}(t)$, $V_{out}(t)$, $I_{out}(t)$, $Q_{out}(t)$, $I_{in}(t)$ and $Q_{in}(t)$ respectively. Then we can define the frequency transfer function for complex input and output signals $V_{in}(j\omega)$ and $V_{out}(j\omega)$ as follows [12]:

$$G_k(j\omega) := \frac{V_{out}(j\omega)}{V_{in}(j\omega)}, \quad (k = 1, 2, 3, 4).$$

Next we derived them explicitly.

2.1 First-order Filter Case

Fact 1 (i) First-order filter transfer function (Fig.1 (a)) is given by

$$G_1(j\omega) = \frac{1 + \omega R_1 C_1}{1 + j\omega R_1 C_1}. \quad (1)$$

(ii) Gain and phase of $G_1(j\omega)$ are given by

$$|G_1(j\omega)| = \frac{|1 + \omega R_1 C_1|}{\sqrt{1 + (\omega R_1 C_1)^2}},$$
$$\tan(\angle G_1(j\omega)) = -\omega R_1 C_1.$$

Figs. 1 (b) and (c) show $|G_1(j\omega)|$ and $\angle G_1(j\omega)$ with regards to ω, respectively.

(iii) The real part ($X_1(\omega)$) and imaginary part ($Y_1(\omega)$) of $G_1(j\omega)$ are given as follows:

$$G_1(j\omega) := X_1(\omega) + jY_1(\omega).$$

$$X_1(\omega) := \frac{1 + \omega R_1 C_1}{\sqrt{1 + (\omega R_1 C_1)^2}},$$

$$Y_1(\omega) := -\frac{(\omega R_1 C_1)(1 + \omega R_1 C_1)}{\sqrt{1 + (\omega R_1 C_1)^2}}.$$

Fig.1 (d) shows the Nyquist chart of $G_1(j\omega)$.

Fact 2 Table 1 shows gain characteristics of $G_1(j\omega)$. Also note that in general, $|G_1(j\omega)| \neq |G_1(-j\omega)|$, and

$$\left[\frac{\partial |G_1(j\omega)|}{\partial \omega}\right]_{\omega=\omega_1} = 0.$$

Table 1: Characteristics of $|G_1(j\omega)|$.

ω	$X_1(\omega)$	$Y_1(\omega)$	$\lvert G_1(j\omega)\rvert$
$-\infty$	-1.0	-1.0	$\sqrt{2}$
$-(1+\sqrt{2})\omega_1$	-0.2	-0.5	1.3
$-\omega_1$	0.0	0.0	0.0
$(1-\sqrt{2})\omega_1$	0.5	0.2	$\sqrt{0.29}$
0.0	1.0	0.0	1.0
$(-1+\sqrt{2})\omega_1$	1.2	0.5	1.3
ω_1	-1.0	-1.0	$\sqrt{2}$
$(1+\sqrt{2})\omega_1$	0.5	-1.2	1.3
∞	-1.0	-1.0	$\sqrt{2}$

Fact 3 Table 2 shows phase characteristics of $G_1(j\omega)$. Also note that $\tan \angle G_1(j\omega) = -\tan \angle G_1(-j\omega)$, but $\angle G_1(j\omega) \neq -\angle G_1(-j\omega)$, and

$$\angle G_1(j\omega) = \begin{cases} -\angle G_1(-j\omega) & (0 \leqq \omega < \omega_1) \\ \angle G_1(-j\omega) - \pi & (\omega_1 < \omega). \end{cases}$$

Table 2: Characteristics of $\angle G_1(j\omega)$.

ω	$X_1(\omega)$	$Y_1(\omega)$	$\angle G_1(j\omega)$
$-\infty$	$= 0$	< 0	$-\pi/2$
$-\infty \sim -\omega_1$	< 0	< 0	$-\pi/2 \sim -(3/4)\pi$
$-\omega_1 - 0$	< 0	< 0	$-(3/4)\pi$
$-\omega_1 + 0$	> 0	> 0	$\pi/4$
$-\omega_1 \sim 0$	> 0	> 0	$\pi/4 \sim 0$
$0 \sim \infty$	> 0	< 0	$0 \sim -\pi/2$
ω_1	> 0	< 0	$-\pi/4$
∞	$= 0$	< 0	$-\pi/2$

Fact 4 (i) Nyquist chart of $G_1(j\omega)$ (Fig.1 (d)) is symmetric with respect to a line of $Y_1 = -X_1$.

(ii) Let decompose G_1 into its real part and imaginary part at $\omega = a\omega_1$ for an arbitrary a ($\neq 0$),

$$G_1(ja\omega_1) := X_1(a\omega_1) + jY_1(a\omega_1).$$

$$\text{Then} \quad G_1(j\frac{1}{a}\omega_1) = -Y_1(a\omega_1) - jX_1(a\omega_1).$$

(iii) $|G_1(ja\omega_1)| = |G_1(j\frac{1}{a}\omega_1)|$.

Proof It follows from eq.(1) that

$$G_1(ja\omega_1) = \frac{1+a}{1+ja} = \frac{1+a}{1+a^2}(1-ja),$$

$$G_1(j\frac{1}{a}\omega_1) = \frac{1+(1/a)}{1+j(1/a)} = \frac{1+a}{1+a^2}(a-j).$$

Then we have Fact 4. (Q.E.D.)

2.2 Second-order Filter Case

Fact 5 (i) Second-order filter transfer function (Fig.2 (a)) is given by

$$G_2(j\omega) = \frac{(1+\omega R_1 C_1)(1+\omega R_2 C_2)}{1 - \omega^2 R_1 C_1 R_2 C_2 + j\omega(C_1 R_1 + C_2 R_2 + 2R_1 C_2)}. \quad (2)$$

(ii) Gain and phase of $G_2(j\omega)$ are given as follows:

$$|G_2(j\omega)| = \sqrt{X_2(j\omega)^2 + Y_2(j\omega)^2}$$
$$= \frac{|1+\omega/\omega_1||1+\omega/\omega_2|}{\sqrt{(1-\omega^2/(\omega_1\omega_2))^2 + \omega^2(1/\omega_1 + 1/\omega_2 + 2/\omega_{12})^2}},$$

$$\tan \angle G_2(j\omega) = \frac{X_2(j\omega)}{Y_2(j\omega)} = \frac{\omega(1/\omega_1 + 1/\omega_2 + 2/\omega_{12})}{\omega^2/(\omega_1\omega_2) - 1}.$$

Fig.2 (b) shows $|G_2(j\omega)|$ with respect to ω, and we see that $G_2(j\omega)$ has zeros at $\omega = -\omega_1, -\omega_2$.

(iii) The real part ($X_2(\omega)$) and imaginary part ($Y_2(\omega)$) of $G_2(j\omega)$ are given as follows:

$$G_2(j\omega) := X_2(\omega) + jY_2(\omega),$$

$$X_2(\omega) := \frac{(1+\omega/\omega_1)(1+\omega/\omega_2)(1-\omega^2/(\omega_1\omega_2))}{(1-\omega^2/(\omega_1\omega_2))^2 + \omega^2(1/\omega_1 + 1/\omega_1 + 2/\omega_{12})^2},$$

$Y_2(\omega) :=$

$$-\frac{\omega(1+\omega/\omega_1)(1+\omega/\omega_2)(1/\omega_1+1/\omega_2+2/\omega_{12})}{(1-\omega^2/(\omega_1\omega_2))^2+\omega^2(1/\omega_1+1/\omega_1+2/\omega_{12})^2}.$$

The Nyquist chart of $G_2(j\omega)$ is given un Fig.2 (c).

Fact 6 Table 3 shows gain characteristics of $G_2(j\omega)$. Also in general $|G_2(j\omega)| \neq |G_2(-j\omega)|$, and

$$\left[\frac{\partial|G_2(j\omega)|}{\partial\omega}\right]_{\omega=\pm\sqrt{\omega_1\omega_2}} = 0.$$

Table 3: Characteristics of $|G_2(j\omega)|$.

ω	$X_2(\omega)$	$Y_2(\omega)$	$\|G_2(j\omega)\|$
$-\infty$	-1.0	0.0	1.0
$-\omega_1$	0.0	0.0	0.0
$-\omega_2$	0.0	0.0	0.0
$-\sqrt{\omega_1\omega_2}$	0.0	$-p$	p
0.0	1.0	0.0	1.0
$\sqrt{\omega_1\omega_2}$	0.0	$-q$	q
ω_1	α	β	γ
ω_2	$-\alpha$	β	γ
∞	-1.0	0.0	1.0

Note that in Table 3,

$$p := \frac{(\sqrt{\omega_1}-\sqrt{\omega_2})^2}{\omega_1+\omega_2+2\omega_{21}}, \qquad q := \frac{(\sqrt{\omega_1}+\sqrt{\omega_2})^2}{\omega_1+\omega_2+2\omega_{21}}$$

$$\alpha := \frac{(\omega_1+\omega_2)(-\omega_1+\omega_2)}{\omega_1^2+\omega_1\omega_2+\omega_2^2+\omega_{12}(\omega_1+\omega_2+\omega_{12})},$$

$$\beta := -\frac{(\omega_1+\omega_2)(\omega_1+\omega_2+2\omega_{12})}{\omega_1^2+\omega_1\omega_2+\omega_2^2+\omega_{12}(\omega_1+\omega_2+\omega_{12})},$$

$$\gamma := \frac{\sqrt{2}(\omega_1+\omega_2)}{\sqrt{\omega_1^2+\omega_2^2+2\omega_{21}(\omega_1+\omega_2+\omega_{21})}}.$$

Fact 7 We have the phase characteristics of $G_2(j\omega)$ in Table 4 by noting that $X_2(\omega)=0$ at $\omega=-\omega_1,-\omega_2,\pm\sqrt{\omega_1\omega_2}$ and $Y_2(\omega)=0$ at $\omega=-\omega_1,-\omega_2,0$. Also note that

$$\tan\theta_a := \frac{\omega_b-\omega_a}{\omega_1+\omega_2+2\omega_{12}}, \quad -\pi<\theta_a<-\frac{\pi}{2}.$$

$$\tan\theta_b := \frac{\omega_a-\omega_b}{\omega_1+\omega_2+2\omega_{12}}, \quad -\frac{\pi}{2}<\theta_b<0.$$

where $\omega_a := \max(\omega_1,\omega_2)$, and $\omega_b := \min(\omega_1,\omega_2)$.

Table 4: Characteristics of $\angle G_2(j\omega)$.

ω	$X_2(\omega)$	$Y_2(\omega)$	$\angle G_2(j\omega)$
$-\infty$	-1	0	π
$-\infty \sim -\omega_a$	<0	>0	$\pi/2 \sim \pi$
$-\omega_a \sim -\sqrt{\omega_1\omega_2}$	>0	<0	$-\pi/2 \sim 0$
$-\sqrt{\omega_1\omega_2} \sim -\omega_b$	<0	<0	$-\pi \sim -\pi/2$
$-\omega_b \sim 0$	>0	>0	$0 \sim \pi/2$
$0 \sim \sqrt{\omega_1\omega_2}$	>0	<0	$-\pi/2 \sim 0$
$\sqrt{\omega_1\omega_2} \sim \infty$	<0	<0	$-\pi \sim -\pi/2$
ω_b	>0	<0	θ_b
ω_a	<0	<0	θ_a
∞	-1	0	$-\pi$

Fact 8 (i) Nyquist chart of $G_2(j\omega)$ (Fig.2 (c)) is symmetric with respect to a line of $X_2=0$.
(ii) For an arbitrary a ($\neq 0$),

$$G_2(ja\sqrt{\omega_1\omega_2}) := X_2(a\sqrt{\omega_1\omega_2})+jY_2(a\sqrt{\omega_1\omega_2}),$$

and then

$$G_2(j\frac{1}{a}\sqrt{\omega_1\omega_2}) = -X_2(a\sqrt{\omega_1\omega_2})+jY_2(a\sqrt{\omega_1\omega_2}).$$

(iii) $|G_2(ja\sqrt{\omega_1\omega_2})| = |G_1(j\frac{1}{a}\sqrt{\omega_1\omega_2})|$.

Proof It follows from eq.(2) that

$$\begin{aligned}&G_2(ja\sqrt{\omega_1\omega_2})\\ &= \frac{(1+a\sqrt{\omega_2/\omega_1})(1+a\sqrt{\omega_1/\omega_2})}{(1-a^2)+ja\sqrt{\omega_1\omega_2}((1/\omega_1)+(1/\omega_2)+(2/\omega_{12}))}\\ &= \frac{(\sqrt{\omega_1}+a\sqrt{\omega_2})(\sqrt{\omega_2}+a\sqrt{\omega_1})}{\sqrt{\omega_1\omega_2}(1-a^2)+ja[\omega_1+\omega_2+(\omega_1\omega_2/\omega_{12})]}.\end{aligned}$$

$$\begin{aligned}&G_2(j\frac{1}{a}\sqrt{\omega_1\omega_2})\\ &= \frac{(\sqrt{\omega_1}+a\sqrt{\omega_2})(\sqrt{\omega_2}+a\sqrt{\omega_1})}{-\sqrt{\omega_1\omega_2}(1-a^2)+ja[\omega_1+\omega_2+(\omega_1\omega_2/\omega_{12})]}.\end{aligned}$$

Then we have Fact 8. (Q.E.D.)

2.3 Third-order Filter Case

Fact 9 (i) Third-order filter transfer function (Fig.3 (a)) is given by

$$G_3(j\omega) = \frac{(1+\omega R_1C_1)(1+\omega R_2C_2)(1+\omega R_3C_3)}{D_{G3}(j\omega)}. \qquad (3)$$

Here $D_{G3}(j\omega) := D_{G3R}(\omega)+jD_{G3I}(\omega)$,

$$\begin{aligned}D_{G3R}(\omega) &:= 1-\omega^2[R_1C_1R_2C_2+R_2C_2R_3C_3\\ &+ R_1C_1R_3C_3+2R_1C_3(R_2C_2+R_2C_1+R_3C_2)],\\ D_{G3I}(\omega) &:= \omega[R_1C_1+R_2C_2+R_3C_3\\ &+ 2(R_1C_2+R_2C_3+R_1C_3)]-\omega^3R_1C_1R_2C_2R_3C_3.\end{aligned}$$

(ii) Gain and phase of $G_3(j\omega)$ are given as follows:

$$|G_3(j\omega)| = \frac{|N_3(\omega)|}{\sqrt{D_{G3R}(j\omega)^2+D_{G3I}(j\omega)^2}}$$

$$\tan(\angle G_3(j\omega)) = -\frac{D_{G3I}(j\omega)}{D_{G3R}(j\omega)}.$$

Fig.3 (b) shows $|G_3(j\omega)|$ with respect to ω, and we see that $G_3(j\omega)$ has zeros at $\omega=-\omega_1,-\omega_2,-\omega_3$.
(iii) The real part ($X_3(\omega)$) and imaginary part ($Y_3(\omega)$) of $G_3(j\omega)$ are given as follows:

$$G_3(j\omega) = X_3(\omega)+jY_3(\omega)$$

$$X_3(\omega) := \frac{N_3(\omega)D_{G3R}(\omega)}{D_{G3R}(j\omega)^2+D_{G3I}(j\omega)^2},$$

$$Y_3(\omega) := -\frac{N_3(\omega)D_{G3I}(\omega)}{D_{G3R}(j\omega)^2+D_{G3I}(j\omega)^2}.$$

Note that $X_3(\omega) = 0$ at $\omega = -\omega_1, -\omega_2, -\omega_3, -\alpha, 0, \alpha$, and $Y_3(\omega) = 0$ at $\omega = -\omega_1, -\omega_2, -\omega_3, -\beta, 0, \beta$, where

$$\alpha := \sqrt{\frac{\omega_1\omega_2\omega_3}{\omega_1 + \omega_2 + \omega_3 + 2(\omega_{31} + \omega_{32} + \omega_{21})}}$$

$$\beta := \sqrt{\omega_1\omega_2 + \omega_2\omega_3 + \omega_1\omega_3 + 2(\omega_1\omega_{32} + \omega_2\omega_{31} + \omega_3\omega_{21})}.$$

Fact 10 Let us consider the case that $R_1 = R_2 = R_3 (= R)$ and $C_1 = C_2 = C_3 (= C)$.

(i) The transfer function is given by

$$G_3(j\omega) = \frac{(1+\omega RC)^3}{1 - 9\omega^2R^2C^2 + j(9\omega RC - \omega^3R^3C^3)}.$$

Table 5 shows its gain, phase, X_3 and Y_3 characteristics.

Table 5: Characteristics of $G_3(j\omega)$ when $R_1 = R_2 = R_3 (= R)$ and $C_1 = C_2 = C_3 (= C)$.

ω	$X_3(\omega)$	$Y_3(\omega)$	$\lvert G_3(j\omega)\rvert$	$\angle G_3(j\omega)$
$-\infty$	0.0	1.0	1.0	$\frac{\pi}{2}$
$(-5-\sqrt{24})\omega_1$	0.4	0.4	$0.4\sqrt{2}$	$\pi/4$
$-3\omega_1$	0.1	0.0	0.1	0.0
$-\omega_1$	0.0	0.0	0.0	N/A
$-\omega_1/3$	0.0	0.1	1	$\frac{\pi}{2}$
$(-5+\sqrt{24})\omega_1$	0.4	0.4	$0.4\sqrt{2}$	$\pi/4$
0	1.0	0.0	1.0	0.0
$\omega_1/3$	0.0	-0.8	0.8	$-\pi/2$
ω_1	0.5	0.5	$\sqrt{2}/2$	$-(3/4)\pi$
$3\omega_1$	-0.8	0.0	0.8	$-\pi$
∞	0.0	1.0	1.0	$\pi/2$

(ii) Nyquist chart of $G_3(j\omega)$ (Fig.3 (c)) is symmetric with respect to the line $Y_3 = X_3$.

(iii) For an arbitrary a $(\neq 0)$, we have

$$G_3(j\frac{a}{RC}) := X_3(\frac{a}{RC}) + jY_3(\frac{a}{RC}),$$

and then $$G_3(j\frac{1}{a}\frac{1}{RC}) = Y_3(\frac{a}{RC}) + jX_3(\frac{a}{RC}).$$

(iv) $|G_3(j\frac{a}{RC})| = |G_3(j\frac{1}{a}\frac{1}{RC})|$.

Proof It follows from eq.(3) that

$$G_3(j\frac{a}{RC}) = \frac{(1+a)^3}{1-9a^2+j(9a-a^2)}$$
$$= \frac{(1+a)^3}{\sqrt{(1-9a^2)^2+(9a-a^3)^2}}[1-9a^2+j(a^3-9a)],$$

$$G_3(j\frac{1}{a}\frac{1}{RC}) = \frac{(1+a)^3}{1-9a^2+j(9a-a^2)}$$
$$= \frac{(1+a)^3}{\sqrt{(1-9a^2)^2+(9a-a^3)^2}}[a^3-9a+j(1-9a^2)].$$

Then we have Fact 10. (Q.E.D.)

2.4 Fourth-order Filter Case

Fact 11 Fourth-order RC polyphase filter transfer function is given by

$$G_4(j\omega) = \frac{(1+\omega R_1C_1)(1+\omega R_2C_2)(1+\omega R_3C_3)(1+\omega R_4C_4)}{D_{4R}(\omega) + jD_{4I}(\omega)}.$$

where $D_{4R}(j\omega) = 1$
$- \omega^2\big[R_1R_2(C_1C_2 + 2C_1C_3 + 2C_1C_4 + 2C_2C_3 + 2C_2C_4)$
$+ R_1R_3(C_1C_3 + 2C_1C_4 + 2C_2C_3 + 4C_2C_4 + 2C_3C_4)$
$+ R_2R_3(C_2C_3 + 2C_2C_4 + 2C_3C_4) + R_3R_4C_3C_4$
$+ R_1R_4(C_1C_4 + 2C_2C_4 + 2C_3C_4) + R_2R_4(C_2 + 2C_3)C_4\big]$
$+ \omega^4R_1R_2R_3R_4C_1C_2C_3C_4,$

$D_{4I}(j\omega) = \omega\big[R_1C_1 + R_2C_2 + R_3C_3 + R_4C_4$
$+ 2R_1C_2 + 2R_1C_3 + 2R_1C_4 + 2R_2C_3 + 2R_2C_4 + 2R_3C_4\big]$
$- \omega^3\big[R_1R_2R_3(C_1C_2C_3 + 2C_1C_2C_4 + 2C_1C_3C_4$
$+ 2C_2C_3C_4) + R_2R_3R_4C_2C_3C_4 + R_1R_2R_4(C_1C_2C_4$
$+ 2C_1C_3C_4 + 2C_2C_3C_4) + R_1R_3R_4(C_1C_3C_4 + 2C_2C_3C_4)\big].$

3. Parasitic Capacitance Effects

Next let us consider the parasitic capacitance and loading capacitance effects. Suppose that a RC polyphase filter is implemented on the integrated circuit and hence its resistors and capacitors have parasitic capacitance to the substrate. Also the polyphase filter has load capacitances at the output nodes; we model its equivalent circuit as shown in Fig.4 (the third-order filter case). Then the transfer functions (G_{pk}, $(k = 1, 2, 3)$) are given as follows:

Fact 12 First-order RC polyphase filter case:

$$G_{p1}(j\omega) := \frac{1+\omega R_1C_1}{1+j\omega R_1(C_1+C_{p1})}.$$

Fact 13 Second-order RC polyphase filter case:

$$G_{p2}(j\omega) := (1+\omega R_1C_1)(1+\omega R_2C_2)/D_{p2}(j\omega).$$

Here $D_{p2}(j\omega) := 1$
$- \omega^2R_1R_2[C_1C_2 + C_1C_{p2} + C_2(C_{p1} + C_{p2}) + C_{p1}C_{p2}]$
$+ j\omega[R_1(C_1 + 2C_2 + C_{p1} + C_{p2}) + R_2(C_2 + C_{p2}).$

Fact 14 Third-order RC polyphase filter case:

$$G_{p3}(j\omega) := \frac{(1+\omega R_1C_1)(1+\omega R_2C_2)(1+\omega R_3C_3)}{D_{p3R}(\omega) + jD_{p3I}(\omega)}.$$

Here $D_{p3R}(\omega) := 1 - \omega^2[R_1R_2(C_1C_2 + 2C_2C_3 + 2C_1C_3$
$+C_1(C_{p2} + C_{p3}) + C_2(C_{p1} + C_{p2} + C_{p3}) + 2C_3C_{p1}$
$+C_{p1}(C_{p2} + C_{p3})) + R_2R_3(C_2C_3 + C_2C_{p3} + C_3(C_{p2} + C_{p3})$
$+C_{p2}C_{p3}) + R_1R_3(C_1C_3 + 2C_2C_3 + C_1C_{p3} + 2C_2C_{p3}$
$+C_3(C_{p1} + C_{p2} + C_{p3}) + (C_{p1} + C_{p2})C_{p3})],$

$$\begin{aligned}D_{p3I}(\omega) := \omega[&R_1(C_1+2C_2+2C_3)+R_2(C_2+2C_3)+2R_3C_3\\&+R_1C_{p2}+R_2(C_{p2}+C_{p3})+R_3C_{p3}]-\omega^3R_1R_2R_3[C_1C_2C_3\\&+C_1C_2C_{p3}+C_1C_3(C_{p2}+C_{p3})+C_2C_3(C_{p1}+C_{p2}+C_{p3})\\&+C_1C_{p2}C_{p3}+C_2(C_{p1}+C_{p2})C_{p3}+C_3C_{p1}(C_{p2}+C_{p3})\\&+C_{p1}C_{p2}C_{p3}].\end{aligned}$$

We see that the parasitic capacitances C_{p1}, C_{p2} and C_{p3} do not change the zero positions of $G_{p1}(j\omega)$, $G_{p2}(j\omega)$ and $G_{p3}(j\omega)$ (which are $\omega = -\omega_1, -\omega_2, -\omega_3$). Fig.5 shows the simulation result of gain characteristics including parasitic capacitances and we see that as the parasitic capacitance values increase, the gain drops for large $|\omega|$.

Acknowledgement We would like to thank T. Kozawa, M. Hotta, T. Tsukada and A. Wada, of STARC which supports this project. Thanks are also due to H. Tanimoto, K. Saijo, H. Sadamura and K. Wilkinson for valuable discussions.

文　　献

[1] M. J. Gingell, "Single Sideband Modulation Using Sequence Asymmetric Polyphase Networks," *Electrical Communication,* vol.48, no.1 and 2, pp.21-25 (1973).

[2] J. Kang, H. Kobayashi, T. Kitahara, S. Takigami and H. Sadamura, "Explicit Analysis of RC Polyphase Filter for I, Q Signal Generation and Image Rejection," *The 15th Workshop on Circuits and Systems in Karuizawa,* pp.53-58 (April 2002).

[3] H. Kobayashi, J. Kang, T. Kitahara, S. Takigami and H. Sadamura," Explicit Transfer Function of RC Polyphase Filter for Wireless Transceiver Analog Front-End, "*2002 IEEE Asia-Pacific Conference on ASICs*, pp.137-140, Taipei, Taiwan (Aug. 2002).

[4] J. Crols and M. Steyeart, *CMOS Wireless Transceiver Design,* Kluwer Academic Publishers (1997).

[5] S. Sheng and R. Broderson, *Low Power Wireless Communication Applications - A Wideband CDMA System Design -* , Kluwer Academic Publishers (1998).

[6] F. Behbahani, Y. Kishigami, J. Leete and A. A. Abidi, "CMOS Mixers and Polyphase Filters for Large Image Rejection," *IEEE J. Solid-State Circuits,* vol.36, no.6, pp.873-887 (June 2001).

[7] A. Rofougaran, G. Chang, J. J. Rael, J. Y.-C. Chang, M. Rofougaran, P. J. Chang, M. Djafari, M.-K.Ku, E. R. Roth, A. A. Abidi and H. Samueli, "A Single-Chip 9–MHz Spread-Spectrum Wireless Transceiver in 1-μm CMOS - Part I; Architecture and Transmitter Design," *IEEE J. Solid-State Circuits,* vol.33, no.4, pp.515-534 (April 1998).

[8] M. Steyeart, M. Borremans, J. Janssens, B. D. Muer, N. Itoh, J. Carnicky, J. Crols, E. Morifuji, H. S. Momose and W. Sansen, "A Single-Chip CMOS Transceiver for DCS-1800 Wireless Communications," *ISSCC Digest of Technical Papers,* vol.41, pp.48-49 (Feb. 1998).

[9] J. Fukura and H. Tanimoto, "Analysis of RC Polyphase Filter Using Multi-Port F-matrix, "*IEEJ Technical Meeting on Electronic Circuits, ECT-02-71*, Kitami (July 2002).

[10] Y. Niki, J. Kang, H. Kobayashi, N. Yamaguchi and T. Kitahara, "Analysis and Design of RC Polyphase Filters - Input Impedacne, Output Termination, Component Mismatch Effects, Flat-Passband Filter Design -", *IEICE Technical Meeting of Circuits and Systems,* Wakayama (Jan. 2003).

[11] L. Cohen, *Time-Frequency Analysis,* Prentice Hall (1995).

[12] J. Crols and M. Steyeart, "Low-IF Topologies for High-Performance Analog Front Ends of Fully Integrated Receivers," *IEEE Trans. on Circuits and Systems II,* vol.45, no.3, pp.269-282 (March 1998).

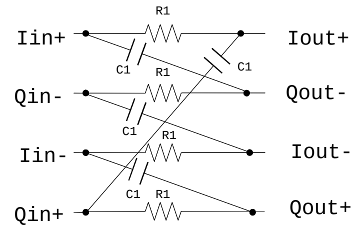

Fig.1 (a) : The first-order RC polyphase filter.

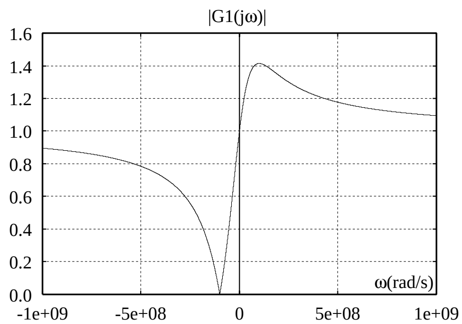

Fig.1 (b) : Gain characteristics of Fig.1 (a).

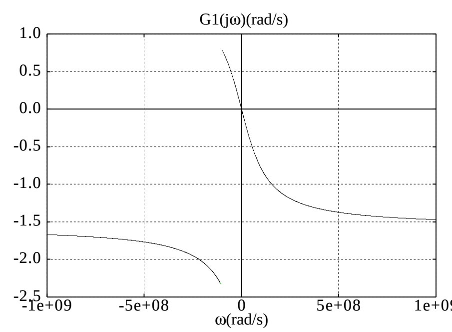

Fig.1 (c) : Phase characteristics of Fig.1 (a).

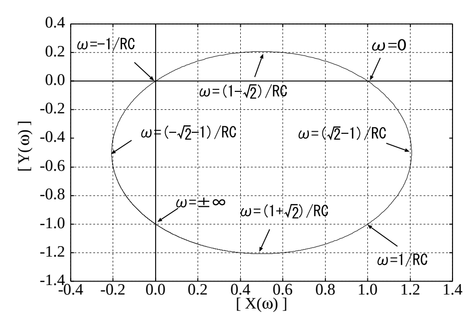

Fig.1 (d) : Nyquist chart of $G_1(j\omega) := X_1(\omega) + jY_1(\omega)$.

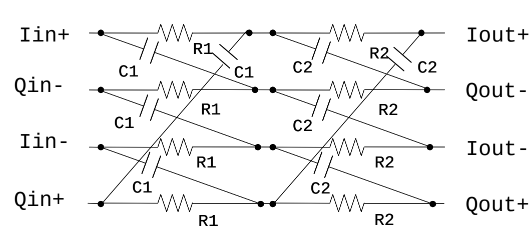

Fig.2 (a) : The second-order RC polyphase filter.

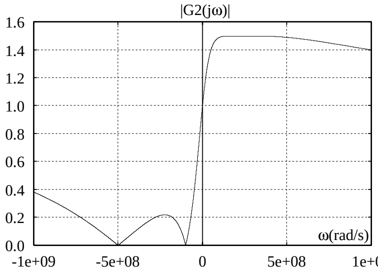

Fig.2 (b) : Gain characteristics of Fig.2 (a) when $R_1 = 1k\Omega, C_1 = 10pF, R_2 = 2k\Omega$ and $C_2 = 1pF$.

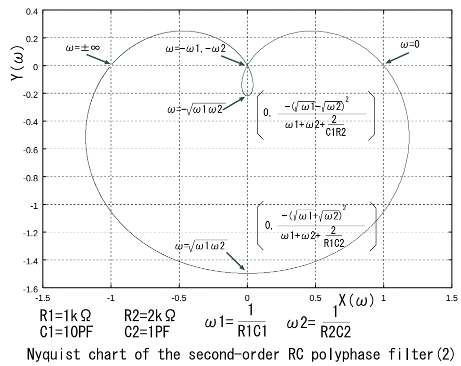

Fig.2 (c) : Nyquist chart of $G_2(j\omega) := X_2(\omega) + jY_2(\omega)$.

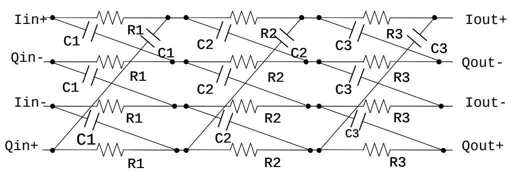

Fig.3 (a) : The third-order RC polyphase filter.

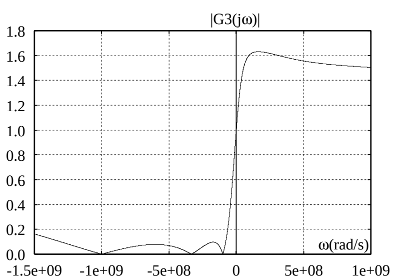

Fig.3 (b): Gain characteristics of the third-order RC polyphase filter when $R_1 = 1k\Omega, C_1 = 10pF$, $R_2 = 3k\Omega, C_2 = 1pF$, $R_3 = 5k\Omega$ and $C_3 = 0.2pF$.

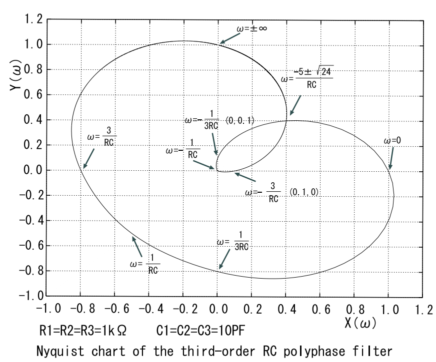

Fig.3 (c) : Nyquist chart of $G_3(j\omega) := X_3(\omega) + jY_3(\omega)$ when $R_1 = R_2 = R_3$ and $C_1 = C_2 = C_3$.

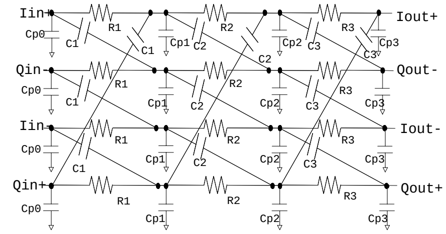

Fig.4: Equivalent circuit of the third-order RC polyphase filter with parasitic capacitance to substrate (C_{p0}, C_{p1}, C_{p2}, and a part of C_{p3}) and load capacitance (the other part of C_{p3}).

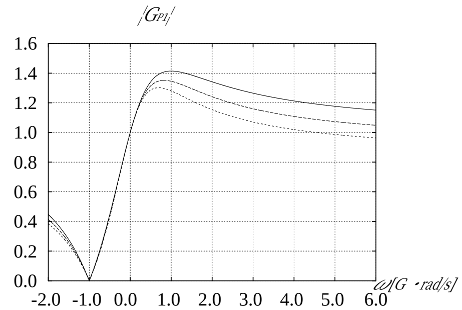

Fig.5 (a) : Gain characteristics of a first-order RC polyphase filter ($R_1 = 1k, C_1 = 1p$) with parasitic capacitances. From the top to bottom lines, $C_{p1} = 0, 0.1p$ and $0.2p$ respectively.

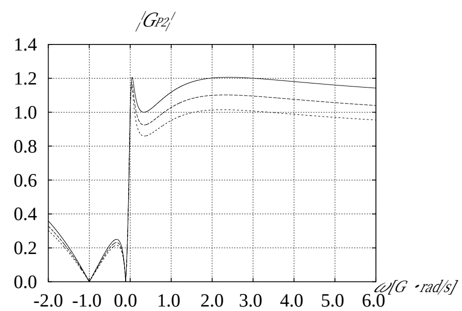

Fig.5 (b) : Gain characteristics of a second-order RC polyphase filter ($R_1 = 1k, R_2 = 3k, C_1 = 1p, C_2 = 3p$) with parasitic capacitances. From the top to bottom lines, $C_{p1}/C_1 = C_{p2}/C_2 = 0, 0.1$ and 0.2 respectively.

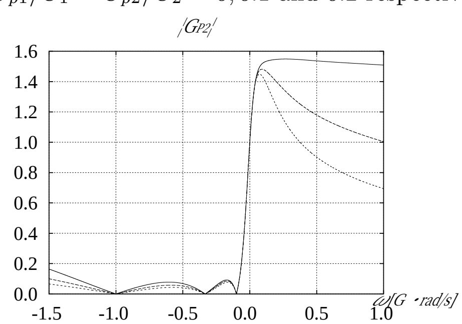

Fig.5 (c) : Gain characteristics of a third-order RC polyphase filter ($R_1 = 1k$, $R_2 = 3k$, $R_3 = 5k$, $C_1 = 1p$, $C_2 = 0.1p$, $C_3 = 0.02p$) with parasitic capacitances. From the top to bottom lines, $(C_{p1}, C_{p2}, C_{p3}) = (0, 0, 0)$, $(0.1p, 0.01p, 0.002p)$ and $(0.2p, 0.02p, 0.004p)$ respectively.